SAR IMAGES RECONSTRUCTION VIA PHASE RETRIEVAL

T. Isernia[1-2], *V. Pascazio*[3], *R. Pierri*[4], *G. Schirinzi*[2]

[1]Dipartimento di Ingegneria Elettronica - Università di Napoli *Federico II*
via Claudio, 21 - 80125 Napoli, Italy
☎: +39-(0)81-7683512; fax: +39-(0)81-5934448; e-mail: isernia@die003.dis.unina.it

[2]Istituto per l'Elettromagnetismo e i Componenti Elettronici - Consiglio Nazionale delle Ricerche
via Diocleziano, 328 - 80124 Napoli, Italy
☎: +39-(0)81-5707999; fax: +39-(0)81-5705734; e-mail: schiri@irecel.irece.na.cnr.it

[3]Istituto di Teoria e Tecnica delle Onde Elettromagnetiche - Istituto Universitario Navale
via Acton, 38 - 80133 Napoli, Italy
☎: +39-(0)81-5513976; fax: +39-(0)81-5512884; e-mail: pascazio@naval.uninav.it

[4]Dipartimento di Ingegneria dell'Informazione - Seconda Università di Napoli
via Roma, 29 - 81031 Aversa (CE), Italy
☎: +39-(0)81-5044035; fax: +39-(0)81-5045804; e-mail: pierri@uxing2.sunap.it

ABSTRACT

A new method to accurately reconstruct a Synthetic Aperture Radar complex image starting from phase errors affected raw received data is presented. It is based on a phase retrieval algorithm, and the unknown complex reflectivity is found by minimising a proper functional using the partial phase information carried out by the phase corrupted raw data as the initial guess of an iterative procedure. The method, which is capable of compensating for both 1-D and 2-D phase errors, has been validated on real data.

1 INTRODUCTION

Phase fluctuations in Synthetic Aperture Radar (SAR) received data can be induced mainly by two factors: propagation at GHz frequencies in turbulent atmosphere and/or troposphere [1] and unwanted deviations from the nominal trajectory of the platform carrying the antenna [2-3]. These phase distortions cause a degradation in performance of the system, producing a blurred image.

In this paper we present a new method to estimate accurately a complex scene imaged by a SAR system starting from phase error affected received data. The method is based on the inversion of the non linear relationship between the raw square amplitude data and the unknown complex reflectivity of the scene, and it uses the partial phase information carried by the phase corrupted raw data. The method is intimately related to the PR of a bandlimited signal from its magnitude distribution [4]. The use of intensity information makes the problem to be solved non linear and ill-posed, so that its solution has to be found by minimising a proper functional. The proposed procedure is independent of the source of phase errors, allowing to compensate for effects that low and high frequency errors on the data induces in the complex image, do not require the presence of strong scatterers in the image, is able to compensate for 1D and 2D phase errors, and acts directly on SAR raw data. These features are not contemporary presented by any other method published in the literature. Note that the overall procedure acts as an image processing technique.

2 SAR IMAGING FROM PHASE CORRUPTED DATA BY A PHASE RETRIEVAL ALGORITHM

The complex signal received by the SAR antenna can be expressed [5] by equation:

$$h(x',r') = \iint \gamma(x,r)\, g(x'-x, r'-r; x, r)\, dx\, dr, \quad (1)$$

where (x,r) and (x',r') are the azimuth and range co-ordinates on the ground and on board, respectively, γ is the complex reflectivity coefficient of the imaged scene, and g is the system space-variant PSF (SVPSF), depending on the electronic, geometrical, and kinematic parameters of the SAR system, whose Fourier transform (the system transfer function needed for the image computing) can be analytically evaluated [5]. The space variance of the PSF takes into account the required variation of the focusing parameters when moving from the near to the far range image points. Due to the nature of the system transfer function, the space variance can be efficiently implemented by operating simple shift operation in the frequency domain [5]. If the scene dimension is sufficiently small [5], the space variance of g can be neglected, and the imaging system acts like a linear filter with a space-invariant PSF (SIPSF); in this case Eqn. (1) reduces to a convolution, so that

$$h(x,r) = [\gamma \otimes g](x,r) = \mathcal{G}\gamma, \quad (2)$$

where $\otimes$ indicates two dimensional convolution, and $\mathcal{G}$ is the linear operator linking the ground reflectivity function to the received data. The extension of the treatment to the SVPSF case is straightforward and requires only a marginal increase in computational complexity [5].

Phase errors on the received signal can greatly affect the accurate focusing of the final image. In particular, it can be shown that if the motion instability of the flying platform is not very large [2-3], only the phase of the received signal is affected, so that the phase perturbed received signal is given by:

$$h_m(x',r') = h(x',r')\ \exp\left[j\vartheta(x',r')\right], \qquad (3)$$

where ϑ represents the phase term induced by motion instability and/or turbulence effects. According to Eqn. (3) the amplitudes of the ideal received signal h and of the phase corrupted received signal h_m are the same, while their phases are different[1]. For this reason, an image focusing technique properly exploiting the magnitude information present in the phase error affected received data is highly desirable. Denoting by $\mathcal{B}$ the operator performing the square amplitude of $\mathcal{G}\gamma$

$$\mathcal{B}\gamma = (\mathcal{G}\gamma)(\mathcal{G}\gamma)^* = |\mathcal{G}\gamma|^2, \qquad (4)$$

where * denotes complex conjugation, it can be stated that

$$\mathcal{B}\gamma = |h|^2 = |h_m|^2. \qquad (5)$$

It has to be noted that the link between the unknown function γ and the data $|h_m|^2$ is non linear.

SAR image focusing amounts to find an estimate of the reflectivity function of the observed scene. In fact, even if the actual reflectivity function γ has an infinite bandwidth (i.e., it does not belong to a finite dimensional space), the finite extension received signal h, by virtue of the nature of $\mathcal{G}$, has an essentially finite bandwidth, so that it belongs to a finite dimensional space. Consequently, starting from h, we can get at most a finite dimensional (i.e., a finite resolution) estimate of γ satisfying Eqn. (5). As the full knowledge of $h = \mathcal{G}\gamma$ would allow conventional SAR processing, problem (5) is analogous to a PR problem for a bandlimited function (h) from its intensity distribution ($|h|^2 = |h_m|^2$). In that case, properties of bandlimited signals allow us to prove that, apart from a phase constant, the only solutions of the problem are the unknown signal and its complex conjugate [4]. In the present case, however, h belongs to the range of $\mathcal{G}$, which is a subset of the set of bandlimited functions, so that, thanks to the nature of g, this latter ambiguity can be removed [6]. However, actual received data are affected by measurement errors. Under this condition, a solution to (7) could not exist at all, so that the inversion has to be performed in a generalised sense, that is, by finding the global minimum of a proper functional. The problem can be recast as finding γ such that

$$\tilde{\gamma} = \arg \min_{\gamma \in \Gamma} \phi(\gamma), \quad \phi(\gamma) = \left\| \mathcal{B}\gamma - |h_m|^2 \right\|^2, \qquad (6)$$

wherein $\|\cdot\|$ denotes the quadratic norm in the space of the data.

3 THE SOLUTION ALGORITHM

The sampling of raw data is usually accomplished according to its bandwidth, whose upper bound is given by the known bandwidth of the system unit response g (see Eqn. (2)). However, the phase error affected raw data h_m has a larger bandwidth so that its reliable sampling implies a finer grid in order to avoid aliasing effects. By virtue of (4) and (5), the available data have twice the bandwidth of phase error free raw data $h = \mathcal{G}\gamma$. If the complex phase error affected data are sampled at the appropriate frequency (i. e., they are well represented by their samples), it is possible to get the intensity data samples at the required sampling frequency through interpolation. Let $|h_m|^2$ the discretised versions of $|h_m|^2$. Moreover, let $\hat{\gamma}$ be a pointwise representation of $\gamma \in \Gamma$, sampled, as usual, at the same rate as h. $\hat{\gamma}$ will have a finite number $M \times N$ of complex samples, where M and N are the extensions along the two dimensions of the image. On the other hand, the system PSF g is an essentially band-limited function of finite extension and can be accordingly approximated by $P \times Q$ discrete complex samples. Consequently, $|h_m|^2$, the data of the inverse problem, can be represented in a space of real dimension $2(M+P) \times 2(N+Q)$.

As a consequence of the above, the entire problem can be accurately approximated in finite dimensional spaces. In particular, operator $\mathcal{B}$ can be evaluated in the finite dimensional space of the data as:

$$\boldsymbol{B}\,\hat{\gamma} = \left|\boldsymbol{G}\,\hat{\gamma}\right|^2 \qquad (7)$$

where $\boldsymbol{G}$ is the discretised version of $\mathcal{G}$.

Note that no similar accurate finite dimensional approximation of the problem is possible when using amplitude [7] (rather than intensity) data. In fact, even assuming bandlimitedness of $\mathcal{G}\gamma$, $|\mathcal{G}\gamma|$ is not band limited, so that it cannot be represented with a finite number of samples.

The discretised problem amounts to finding $\hat{\gamma}$ such that

$$\phi(\hat{\gamma}) = \sum_{l=1}^{2(M+P)} \sum_{s=1}^{2(N+Q)} \left(\boldsymbol{B}\,\hat{\gamma}\big|_{ls} - \left|\hat{h}_m(l,s)\right|^2 \right)^2 \qquad (8)$$

is globally minimised with respect to $\hat{\gamma}$.

Thanks to the chosen formulation, several consequences relevant to an accurate minimisation of ϕ can be drawn. First, thanks to the quadratic nature of $\mathcal{B}$, whenever the ratio between the essential dimension of the space of data (related to the bandwidth of $|h|^2$) and the essential dimension of the unknowns (related to the bandwidth of $\hat{\gamma}$) is sufficiently large, it can be argued [8] that local minima problems can be overcome, so that *local* (non random) minimisation schemes can be herein utilised with global effectiveness. In fact, as ϕ is the square distance between the range of $\mathcal{B}$ and the data point, the possible occurrence of local minima is related to the "flatness" of the range of $\mathcal{B}$. The flatter this range is (tending to a plane in the most favourable case), the less likely is the occurrence of local minima. It has been proved in [8] that for quadratic operators of this kind the larger is the dimension of the space of data with respect to the dimension of the unknowns, the flatter the manifold representing the range of $\mathcal{B}$ in such a space, with beneficial effects on the local minima problem. In our case, as $\mathcal{G}$ is a convolution operator, the essential dimension of data is more than doubled with respect to the dimension of γ so that the occurrence of local minima is not very likely.

Moreover, partial information about the phase is available in our case. In fact, starting from the knowledge of phase corrupted received data h_m, we can determine the initial guess of the iterative procedure by the linear inversion of (2):

$$\hat{\gamma}^{(0)} = \boldsymbol{G}^{-1}\hat{h}_m, \qquad (9)$$

[1] Note that, by virtue of the phase term $\exp[j\vartheta]$, h_m has a bandwidth larger than that of h.

where $\boldsymbol{G}^{-1}$ can be analytically evaluated [5]. Processing (9) will provide defocused or blurred images, which, on the basis of the experiments presented in the following Section, will belong, under common conditions, to the attraction region of the global minimum of (8), so that the occurrence of local minima is avoided.

Finally, improved accuracy can be obtained in the neighbourhood of the solution by modifying the functional ϕ through the introduction of weights enhancing the low data values [8], i. e., through the minimisation of the functional

$$\psi(\hat{\gamma}) = \sum_{l=1}^{2(M+P)} \sum_{s=1}^{2(N+Q)} \frac{1}{\left|\hat{h}_m(l,s)\right|^2} \left(\boldsymbol{B}\hat{\gamma}\big|_{ls} - \left|\hat{h}_m(l,s)\right|^2 \right)^2 \quad (10)$$

In order to overcome possible overflow problems, when values $\left|\hat{h}_m(l,s)\right|^2$ are lower than a threshold μ, they are replaced by μ (a fixed amount depending on the numerical precision of the used computer) in the corresponding denominators.

For the minimisation of (8), resort can be made to an iterative scheme of the kind

$$\hat{\gamma}^{(k+1)} = \hat{\gamma}^{(k)} + \lambda_k \underline{\underline{A}}_k \nabla\phi_k . \quad (11)$$

wherein k and $(k+1)$ denote respectively the k-th and $(k+1)$-th iteration. $\nabla\phi$ is given by:

$$\nabla\phi = \boldsymbol{G}^{+}\left[\boldsymbol{G}(\hat{\gamma}) \cdot \left(\left|\boldsymbol{G}(\hat{\gamma})\right|^2 - \left|\hat{h}_m\right|^2 \right) \right], \quad (12)$$

where $\boldsymbol{G}^{+}$ is the adjoint matrix operator of $\boldsymbol{G}$, and λ_k is a scalar factor whose value has to be chosen, at each step, in order to guarantee the maximum decrease along the direction defined by $\underline{\underline{A}}\,\nabla\phi$. The matrix $\underline{\underline{A}}$, finally, determines the kind of minimisation scheme which is in order. We adopt the Polak-Ribiere scheme, a suitable compromise between accuracy and computational complexity. It is worth noting that in all cases $\nabla\phi$ can be efficiently computed through FFT and zero padding operations. Furthermore, the quadratic nature of $\boldsymbol{B}$ allows the step λ_k to be chosen analytically by solving a third degree equation [8], so that the whole minimisation procedure can be efficiently realised. Only slight modifications occur when (10) is used in place of (8).

4 SAR IMAGING EXPERIMENTS

Typical numerical results on actual data are now presented. All the experiments have been obtained by sequentially minimising functional (8) and (10). In agreement with the arguments in [8], this choice exhibited the best performance from the point of view of the reconstructions.

The experiments have been performed on raw data from the German airborne Experimental-SAR (E-SAR). An image of 1550×768 samples, obtained by processing the available actual data is shown in Fig. 1.a. Since the system impulse response function is represented by 450×256 samples, 2048×1024 raw data samples and 4096×2048 intensity data samples, are required. The image obtained by processing the same data corrupted by the 1D 10-th order polynomial phase of Fig. 2 is presented in Fig. 1.b, while the recovered image is presented in Fig. 1.c.

Figure 1.a: *Intensity of a SAR image relative to the E-SAR mission: the image dimension is* $N \times M = 1,550 \times 768$

Figure 1.b: *Intensity of the SAR image obtained by corrupting the raw data of the SAR image of Fig. 1.a with the phase of Fig. 2*

Figure 1.c: *Intensity of the SAR image reconstructed from the phase corrupted raw data of the image of Fig. 1.b*

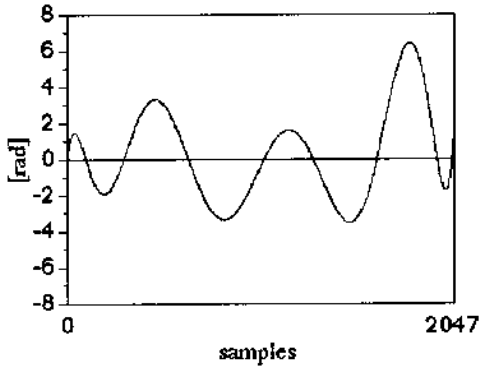

Figure 2
Tenth order polynomial phase used to corrupt the raw data relative to the image of Fig. 1.a

The reconstructions exhibit excellent quality. Note that the degradation effects due to polynomial-like errors primarily cause image defocusing. The defocusing effect along the azimuth direction is evident. It is useful to focus the attention on one of the point targets present in the image, so that cuts across the same part of the three images of Fig. 1 are presented in Fig. 3, where ideal, defocused, and reconstructed point target are represented with solid, dashed, and dotted lines, respectively. Note that the dotted line is hardly visible, thus indicating an almost perfect reconstruction.

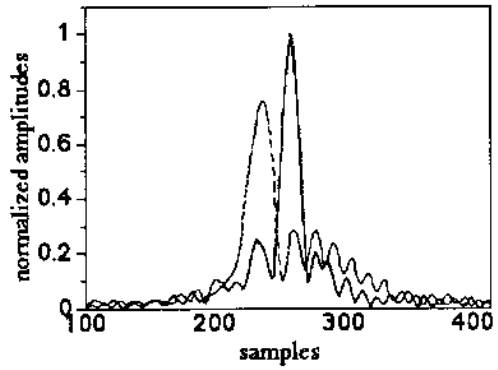

Figure 3
Cuts through the point target present in Fig. 1: actual (solid line), defocused (dashed line), reconstructed (dotted line) point target

Other experiments related to random phase errors were also presented in Ref. [9]: the reconstructions were very good, even if the magnitude of the phase errors was considerable.

As far as the phase of the reconstructed signal is concerned, simulated experiments, showing the capability to perfectly retrieve also the signal phase, were presented in Ref. [9].

It has to be noted that the lack of compensation of these phase effects can be critical for those applications requiring an accurate knowledge of the phase, as for instance in interferometric applications, where the phase of the involved signals are used to reconstruct the elevation of scene under investigation..

5 CONCLUSIONS

We have presented a method that allows to reconstruct a complex SAR image starting from raw data affected by phase errors. The proposed PR based processing technique aims to invert the non linear relationship between the unknown reflectivity of the scene and the raw intensity data. Unlike other PR based approaches [2], that can be considered as post-processing techniques, the proposed procedure acts directly on SAR raw data. The approach is capable of compensating for different kinds of phase errors, both 1D and 2D, unlike other techniques that are based on the assumption that the phase errors depend only on the azimuth co-ordinate. Moreover, uniqueness of a solution can be desumed and important considerations on the local minima problem can be made. Finally, it has also been shown that the initial information carried by the phase corrupted data can be usefully employed in order to profitably start the minimisation procedure. In fact, under common conditions, this point belongs to the attraction region of the required solution.

The main limitations of the method are a slight increase in the required sampling frequency, to well represent the phase corrupted data that have a slightly increased bandwidth respect to the nominal one, and the computer time which is anyway dependent on the amount of phase errors which is present on the data.

The reconstructed images exhibit very high quality when compared with the corresponding ideal ones, and the iterative processing, although we deal with *millions* of data and unknowns, can be performed via FFT and zero padding operations.

REFERENCES

[1] R. L. Fante, "Turbulence-Induced Distortion of Synthetic Aperture Radar Images", *IEEE Trans. Geosci. Remote Sens.*, **GE-32**, pp. 958-961, 1994.

[2] T. Isernia, V. Pascazio, R. Pierri, G. Schirinzi, "Image Reconstruction from Fourier Transform Magnitude with Application to SAR Imaging", *J. Opt. Soc. Am. A.*, **13**, 1996.

[3] V. Pascazio, G. Schirinzi, "An Accurate Model for "Boom"-Motion Induced Phase Errors in SIR-C/X-SAR Interferometric Synthetic Aperture Radar", submitted.

[4] I. Sabba Stefanescu, "On the Phase Retrieval Problem in Two Dimensions", *J. Math. Phys.*, **26**, pp. 2141-2160, 1985.

[5] G. Franceschetti, R. Lanari, V. Pascazio, G. Schirinzi, "WASAR: a Wide Angle SAR Processor", *Proc. IEE Part F*, **139**, pp. 107-114, 1992.

[6] T. Isernia, G. Leone, R. Pierri, "Unique Phase Reconstruction of Near Fields over Planes", in print on *Optics Communications*, 1996.

[7] J. R. Fienup, "Phase Retrieval Algorithm: a Comparison", *Applied Optics*, **21**, 2758-2769, 1982.

[8] T. Isernia, G. Leone, R. Pierri, F. Soldovieri,"On the Local Minima in Phase Reconstruction Algorithms", in print on *Radio Science*, 1996.

[9] T. Isernia, V. Pascazio, R. Pierri, G. Schirinzi, "Synthetic Aperture Radar Imaging from Phase Corrupted Data", in print on *IEE Proc. - Radar, Sonar Navigat.*, 1996.